Acetylcholine Modulates Respiratory Pattern: Effects Mediated by M3-Like Receptors in PreBötzinger Complex Inspiratory Neurons

X. M. Shao and **J. L. Feldman**

Department of Neurobiology, University of California, Los Angeles, California 90095-1763

Abstract

Perturbations of cholinergic neurotransmission in the brain stem affect respiratory motor pattern both in vivo and in vitro; the underlying cellular mechanisms are unclear. Using a medullary slice preparation from neonatal rat that spontaneously generates respiratory rhythm, we patch-clamped inspiratory neurons in the preBötzinger complex (preBötC), the hypothesized site for respiratory rhythm generation, and simultaneously recorded respiratory-related motor output from the hypoglossal nerve (XIIn). Most (88%) of the inspiratory neurons tested responded to local application of acetylcholine (ACh) or carbachol (CCh) or bath application of muscarine. Bath application of 50 μM muscarine increased the frequency, amplitude, and duration of XIIn inspiratory bursts. At the cellular level, muscarine induced a tonic inward current, increased the duration, and decreased the amplitude of the phasic inspiratory inward currents in preBötC inspiratory neurons recorded under voltage clamp at −60 mV. Muscarine also induced seizure-like activity evident during expiratory periods in XIIn activity; these effects were blocked by atropine. In the presence of tetrodotoxin (TTX), local ejection of 2 mM CCh or ACh onto preBötC inspiratory neurons induced an inward current along with an increase in membrane conductance under voltage clamp and induced a depolarization under current clamp. This response was blocked by atropine in a concentration-dependent manner. Bath application of 1 μM pirenzepine, 10 μM gallamine, or 10 μM himbacine had little effect on the CCh-induced current, whereas 10 μM 4-diphenylacetoxy-*N*-methylpiperidine methiodide blocked the current. The current-voltage (*I-V*) relationship of the CCh-induced response was linear in the range of − 110 to −20 mV and reversed at −11.4 mV. Similar responses were found in both pacemaker and nonpacemaker inspiratory neurons. The response to CCh was unaffected when patch electrodes contained a high concentration of EGTA (11 mM) or bis-(*o*-aminophenoxy)-*N,N,N′,N′*-tetraacetic acid (10 mM). The response to CCh was reduced greatly by substitution of 128 mM Tris-Cl for NaCl in the bath solution; the *I-V* curve shifted to the left and the reversal potential shifted to −47 mV. Lowering extracellular Cl⁻ concentration from 140 to 70 mM had no effect on the reversal potential. These results suggest that in preBötC inspiratory neurons, ACh acts on M3-like ACh receptors on the postsynaptic neurons to open a channel permeable to Na^+ and K^+ that is not Ca^{2+} dependent. This inward cation current plays a major role in depolarizing preBötC inspiratory neurons, including

pacemakers, that may account for the ACh-induced increase in the frequency of respiratory motor output observed at the systems/behavioral level.

Introduction

ACh is involved in central respiratory control (Burton et al. 1994, 1995; Gesell et al. 1943; Gillis et al. 1988; Metz 1958; Murakoshi et al. 1985; Nattie and Li 1990; Weinstock et al. 1981), including central chemosensitivity (Burton et al. 1997; Dev and Loeschcke 1979; Fukuda and Loeschcke 1979; Gonsalves and Borison 1980; Haxhiu et al. 1984; Monteau et al. 1990; Nattie et al. 1989). Defects in the ventral medullary muscarinic system may play a role in disorders of respiratory control such as sudden infant death syndrome (SIDS) (Kinney et al. 1995a). Central cholinergic mechanisms contribute to respiratory failure caused by organophosphate poisoning (Lotti 1991). Muscarinic receptor subtypes are distributed across brain stem respiratory regions including the ventrolateral medulla (Kinney et al. 1995b; Mallios et al. 1995). Perturbations of ACh synthesis, release, degradation, or activation of ACh receptors in the brain stem result in perturbations of respiratory pattern both in vivo (Foutz et al. 1987; Gillis et al. 1988; Nattie and Li 1990) and in vitro in an en bloc brain stem-spinal cord preparation in neonatal rats (Burton et al. 1994, 1995; Monteau et al. 1990; Murakoshi et al. 1985). The activity of medullary respiratory-related neurons are altered by ACh and cholinergic agonists or antagonists (Böhmer et al. 1987, 1989; Bradley and Lucy 1983; Haji et al. 1996; Jordan and Spyer 1981; Kirsten et al. 1978). The cellular and synaptic mechanism of ACh actions and how this cellular process relates to the behavioral changes in ventilation is not understood.

The preBötzinger complex (preBötC) in the rostroventrolateral medulla is hypothesized as the site for respiratory rhythm generation in mammals (Rekling and Feldman 1998; Smith et al. 1991). There have been accumulating data supporting this hypothesis (Connelly et al. 1992; Funk et al. 1993; Johnson et al. 1994; Koshiya and Guyenet 1996; Koshiya and Smith 1999; Ramirez et al. 1996, 1998; Schwarzacher et al. 1995; Solomon et al. 1999). In earlier studies of the role of cholinergic neurotransmission in central chemosensitivity, cholinergic agents were applied locally to the ventral medullary surface (Dev and Loeschcke 1979; Haxhiu et al. 1984; Nattie et al. 1989), intravenously, or intracerebroventricularly (Burton et al. 1997; Gonsalves and Borison 1980) to anesthetized mammals or by perfusion of the en bloc brain stem-spinal cord preparation in vitro (Monteau et al. 1990). Because the preBötC is located close to the ventral medullary surface, it is difficult to distinguish the direct effects of the agents on preBötC neurons or secondary effects through, for example, nearby (putative) central chemoreceptive areas. Results based on extracellular recording combined with ionophoretic administration of cholin-ergic agents in vivo have been controversial due to the variability (or lack of precise information) concerning recording locations and the states of anesthesia (Böhmer et al. 1987, 1989; Bradley and Lucy 1983; Foutz et al. 1987; Jordan and Spyer 1981; Kirsten et al. 1978; Salmoiraghi and Steiner 1963). Using a medullary slice from neonatal rat that generates respiratory-related motor output, we can locate the preBötC precisely (Gray et al. 1999) and without anesthetic interference, then patch-clamp physiologically classified respiratory neurons and record the system motor output simultaneously in well-controlled conditions, and the tissue is highly accessible for

pharmacological manipulation. In this paper, we address the following questions: which kinds of preBötC neurons, if any, are affected by ACh? How does ACh modulate the activity of these cells? What receptors mediate the ACh effects? What is the relationship between the ACh effects on respiratory neurons and its effects on the respiratory-related motor pattern? We illustrate the ACh effects on respiratory-related motor pattern and identify the underlying synaptic and ionic mechanisms; we also illustrate the ACh receptor pharmacology in preBötC inspiratory neurons including pacemaker neurons. Preliminary data have been published in abstract form (Shao and Feldman 1998).

Methods

Slice preparation

Experiments were performed on a medullary slice preparation that retains functional respiratory networks and generates respiratory rhythm (Smith et al. 1991). Briefly, Sprague-Dawley neonatal rats (0- to 3-days old) were anesthetized by hypothermia (by incubating on ice for $\sim$3–4 min.) and decerebrated. The neuraxis was isolated with care to preserve the XIIn roots, and the cerebellum was removed. The brain stem was pinned down and mounted in the specimen vise of a Vibratome (VT100, Technical Products International) oriented vertically with rostral end upward. The brain stem was sectioned serially in the transverse plane under a dissection microscope until the landmarks at the rostral boundary of preBötC were visible. One transverse slice (550- to 650-μm thick) was cut. The slice was transferred to a recording chamber of 3 ml volume and stabilized with a threaded frame. The dissection and slicing were performed in an artificial cerebrospinal fluid (ACSF) plus 1.0 mM ascorbic acid bubbled with 95% O_2-5% CO_2 at room temperature. The ACSF contained (in mM) 128 NaCl, 3.0 KCl, 1.5 $CaCl_2$, 1.0 $MgSO_4$, 23.5 $NaHCO_3$, 0.5 NaH_2PO_4, and 30 glucose. During electrophysiological recording, the slice was continuously superfused ($\sim$3 ml/min) with ACSF with increased KCl (9 mM) that was recycled into a 200-ml reservoir equilibrated with 95% O_2-5%CO_2 at 26–27°C. All slices had rhythmic activities from the XIIn that were similar in frequency and in temporal pattern to the respiratory activities recorded from en bloc brain stem-spinal cord preparations (Smith et al. 1991).

Electrophysiological recording

Neurons within 100 μm from the upper surface of the slice are visualized readily with infrared-differential interference contrast (IR-DIC) microscopy (×400, Axioskop, Zeiss), and the nucleus ambiguus is identified easily (Rekling and Feldman 1997). The inspiratory neurons we recorded fired in phase with the inspiratory bursts from XIIn were located ventral to the nucleus ambiguus about halfway between the ventral surface of the slice and the nucleus ambiguus. Patch electrodes were pulled from thick-wall (0.32 mm) borosilicate glass on a horizontal puller (Model P-97, Sutter Instruments). The tip size was $\sim$1–1.5 μm (resistance: 4–6.5 MΩ). The electrode filling solution contained (in mM) 140 potassium gluconate, 5.0 NaCl, 0.1 $CaCl_2$, 1.1 EGTA, and 2.0 ATP (Mg^{2+} salt), pH adjusted to 7.3 with KOH. In some experiments, the EGTA concentration of the patch electrode filling solution was raised to 11 mM [or EGTA substituted by 10mMbis-(*o*-aminophenoxy)-*N,N,N ′,N′*-tetraacetic acid (BAPTA)] and the concentration of $CaCl_2$ was raised to 1 mM (high EGTA solution). The electrode was mounted on a hydraulic micromanipulator. Positive

pressure of 100–150 mmHg was applied to the back of the electrode as it was advanced. When the electrode was positioned on the soma surface of the target neuron, positive pressure was released, and negative pressure was applied to form a gigaohm seal. The cell then was ruptured with short negative pressure pulses and/or with a voltage pulse produced by the patch-clamp amplifier. Intracellular signals were amplified with this amplifier (AXOPATCH 200A, Axon Instruments); whole cell capacitance was compensated, as was the series resistance (85–95%). A – 10-mV junction potential was determined experimentally; reported values of potential are corrected values.

Respiratory-related nerve activity was recorded from the cut ends of XIIn roots with a suction electrode, amplified 10,000–20,000 times and band-pass filtered (3–3000 Hz) with an amplifier (Model P511K, GRASS Instrument). Signals from intracellular recording and from XIIn roots were recorded on videocassettes via pulse code modulation (Vetter Instruments). Selected segments of intracellular signals were low-pass filtered with an eight-pole Bessel filter (Frequency Device) and XIIn nerve activity was rectified and low-pass filtered (Paynter filter, $\tau = 15$ ms), then digitized with DIGIDATA 1200 hardware and CLAMPEX 7 software (Axon Instrument) on a Pentium computer on-or off-line.

Data were analyzed with pCLAMP (Axon Instrument) or ORIGIN (V5, Microcal Software) software. Averaged data are presented as means ± SD except the cases indicated with means ± SE, n = number of cells (for whole cell recording) or preparations (for XIIn motor output recording) are indicated. Paired t-tests were used taking the electrophysiological measurements during pharmacological manipulation versus those in control conditions in the same cell or same preparation; P 0 05 was the criterion for statistical significance.

In experiments in which Cl⁻ concentration was changed, a 3 M KCl-agar bridge was used for grounding the bath solution to avoid variation in junction potential between the bath solution and the AgCl grounding probe.

Drug application

Drugs were applied either by adding to the bath solution or by local pressure ejection. Single- or double-barrel pressure ejection micropipettes were mounted on a hydraulic micromanipulator, and the tip size of the ejection pipette was ∼1–1.5 μm for each barrel with ∼8–10 psi pressure applied to the back of the pipette. The ejection pipettes were positioned in the tissue ∼30–40 μm away from the soma of the recorded neurons under an IR-DIC microscope. The space clamp problem inherent to voltage clamping in slice preparations was minimized by applying agonists in this way because the current elicited was spatially restricted to the soma or proximal dendrites, which were well clamped. Drugs were dissolved in a pipette solution containing (in mM) 150 NaCl, 9 KCl, 1.5 CaCl$_2$, 1.0 MgSO$_4$, 10 HEPES, and 30 glucose, pH adjusted to 7.4 with NaOH. In experiments in which the ionic components of the bath solution were changed (e.g., low Na⁺ solution), the composition of the pipette solution also changed correspondingly. Because the ejection pipette tip was small and in the tissue, the concentration of the locally applied drugs was not homogenous around the neuron. The drug concentration at the cell was estimated to be much lower than that in the pipette. We used higher concentrations (10 times higher than that one would use for isolated cells) in the pipette to ensure eliciting responses.

Cholinergic agents pirenzepine dihydrochloride, gallamine triethiodide, 4-diphenylacetoxy-*N*-methylpiperidine methiodide (4-DAMP) were obtained from RBI. (+)-Himbacine, (−)-atropine sulfate, ACh-chloride, carbachol, (+)-muscarine chloride, (−)-nicotine (hydrogen tartrate salt), and tetrodotoxin were obtained from Sigma.

Results

Ninety-two preBötC inspiratory neurons in 75 slice preparations were examined. Inspiratory neurons exhibit periodic bursts of action potentials (under current clamp) or periodic inward currents (under voltage clamp) in phase with the inspiratory burst activities of XIIn. Eighty-one (88%) of these inspiratory neurons responded to local application of 2 mM ACh or CCh or bath application of 50 μM muscarine.

Bath application of 50 μM muscarine increased the respiratory frequency by $50.3 \pm 33.5\%$, increased inspiratory duration by $109.5 \pm 90.1\%$, and increased the amplitude of integrated inspiratory bursts fromXIInby $34.0 \pm 31.6\%$ (Table 1). In inspiratory neurons, 50 μM muscarine induced a tonic inward current (21.5 ± 20.4 pA, $n = 6$), increased the duration of the phasic inspiratory inward currents by $66.6 \pm 59.9\%$,and decreased the amplitude by $39.4 \pm 14.0\%$ in inspiratory neurons (Fig. 1 A, a–c) under voltage clamp at −60 mV (Table 1). Muscarine depolarized inspiratory neurons under current clamp. Muscarine also induced seizure-like activity apparent during the expiratory periods (Fig. 1B, raw signal from XIIn). Notice that there was no corresponding activity in inspiratory neurons during the seizure-like activity of XIIn (Fig. 1B). Similar responses also were observed in pacemaker neurons ($n = 3$, see following text). Both the motor output of the system, i.e., XIIn activity, and the activity of the inspiratory neurons recovered after bath application of 10 μM atropine (Fig. 1A). Muscarine increased the number of action potentials from 14.7 ± 7.7 to 18.4 ± 8.7 per inspiratory period under current clamp (Fig. 1C) but did not change the number of action potentials per depolarizing current pulse applied during the expiratory period (40 pA, 500 ms; Fig. 1D, Table 1). This suggests that the muscarine-induced increase in number of action potentials per inspiratory drive resulted primarily from the increased duration of inspiratory drives. Inspiratory neurons did not exhibit adaptation during depolarizing current pulses in either control conditions or during muscarine application ($n = 6$).

In the presence of TTX (0.5–1.0 μM), local application of 2 mM ACh or CCh with a short pressure pulse (∼200–250 ms) induced a slowly activating and long-lasting (12.2 ± 3.2 s) inward current (43.2 ± 26.4 pA, $n = 12$) with an associated increase in whole cell current noise and membrane conductance (Fig. 2B). The profile of the response inward current did not change significantly during an 1-h recording period. The response slightly desensitized with a long application (10 s) of ACh (Fig. 2A). The desensitization was observed in both ACh- and CCh-induced responses. This inward current was blocked by atropine in a concentration-dependent manner ($n = 7$) and partially recovered after perfusion with standard recording solution (Fig. 2B). Local application of 0.5 or 1 mM nicotine in identical conditions (double-barrel ejection pipette, one with ACh and the other with nicotine) did not induce similar response (data not shown). These results, taken together, suggest that there are muscarinic receptors on preBötC inspiratory neurons and that the excitatory effect of ACh was mediated primarily by muscarinic receptors that open channels.

Pacemaker neurons are a subset of inspiratory neurons that have voltage-dependent endogenous bursting properties, i.e., "pacemaker-like properties." They normally fire during inspiratory bursts but also can be induced to fire rhythmic bursts during expiratory periods when current is injected to keep the membrane voltage at −45 to −55 mV (q.v., Smith et al. 1991). Figure 3A shows a pacemaker and a nonpacemaker inspiratory neuron. In the presence of 0.5–1.0 μM TTX, local application of 2 mM CCh induced virtually identical responses in these neurons under voltage clamp at −60 mV (Fig. 3B). Selected traces of whole cell currents elicited by hyperpolarizing and depolarizing voltage-clamp pulses (−110, −40, and −10 mV, 200 ms) in control and during local application of CCh are shown in Fig. 3C, i and ii. Subtraction of the elicited current during CCh from that of control gives the net effects of CCh (Fig. 3Ciii). The *I-V* relationships of the CCh-induced responses were very similar between pacemaker and nonpacemaker inspiratory neurons (Fig. 3D).

The M3 muscarinic receptor antagonist 4-DAMP (10 μM) blocked the CCh (2 mM, pressure ejection)-induced inward current in inspiratory neurons under voltage clamp at −60 mV (bath solution contained 0.5 μM TTX). There was partial recovery after a 10-min wash with standard recording solution (Fig. 4A). Because 4-DAMP is not very specific for the M3 receptor subtype (Dörje et al.1991), we tested three other antagonists: M1 antagonist pirenzepine (PZ, 1 μM), M2 antagonist gallamine (10 μM), and M2/M4 antagonist himbacine (10 μM, Fig. 4A). They had little effect on the CCh-induced inward current compared with control. Figure 4C shows a summary of antagonist effects on the amplitude of the CCh- induced inward current. 4-DAMP decreased this current by $83.4 \pm 10.5\%$ (from 32.9 ± 21.5 to 4.7 ± 2.9 pA, paired *t*-test, $P = 0.021$, $n = 6$). The effects of PZ (paired *t*-test, $P = 0.338$, $n = 6$), gallamine ($P = 0.581$, $n = 3$), or himbacine ($P = 0.144$, $n = 5$) were not statistically significant. Taken together, these results suggest that CCh induced a 4-DAMP-sensitive current in preBötC inspiratory neurons that is not mediated by M1, M2, or M4 receptors. It is most likely mediated by M3-like acetylcholine receptors. The effects of 4-DAMP were the same in pacemaker (Fig. 4B) and nonpacemaker inspiratory neurons. On the basis of this and the previous observations (Fig. 3), we assume that ACh acts on the same muscarinic receptor subtype and ionic channels in both pacemaker and nonpacemaker inspiratory neurons, and therefore we pooled the data from these neurons in the following experiments.

To investigate whether the CCh-induced response is Ca^{2+} dependent, we recorded the CCh-induced inward current with whole cell patch electrode containing a high concentration of EGTA (11 mM EGTA) or BAPTA (10 mM). The mean current amplitude was 39.9 ± 18.3 pA and mean duration was 12.9 ± 4.0 s ($n = 11$). There was no significant difference compared with controls with low EGTA patch electrodes (43.2 ± 26.4 pA and 12.2 ± 3.2 s, $n = 12$, $P = 0.74$ and 0.66, respectively).

The steady-state *I-V* relationship of preBötC inspiratory neurons was obtained by applying a series of 200-ms voltage pulses from a holding potential of −65 mV to a range from −110 to 0 mV. Local application of CCh increased the slope of the *I-V* curve. The *I-V* curve during application of CCh and that of the control intersected at about −10 mV (Fig. 5A). The *I-V* relationship of the response induced by local application of CCh was determined by subtracting the steady-state *I-V* curve in control conditions from that during application of

CCh (Figs. 5B and 3C). The *I-V* curves were linear in the voltage range of −110 to −20 mV, and the reversal potential E_{CCh}, determined by extrapolation of the linear regression line, was −11.4 mV (Fig. 5B, mean *I-V* curve of 18 inspiratory neurons). In a bath solution containing a low-Na^+ solution (128 mM of NaCl was substituted by equimolar Tris-Cl; the remaining Na^+ concentration was 24 mM), the CCh-induced inward current under voltage clamp at −65 mV was reduced greatly, and it partially recovered after switching back to standard recording solution (Fig. 6A). This suggests that CCh opens a channel permeable to Na^+. Because the CCh-induced current reversed at about − 11 mV, between the equilibrium potentials of Na^+ (E_{Na}) and K^+ (E_k), we assumed the channel was permeable to both Na^+ and K^+. According to the equation derived by Goldman (1943) and Hodgkin and Katz (1949), the permeability ratio of K^+ to Na^+ can be calculated

$$P_k/P_{Na} = ([Na^+]_o - [Na^+]_i \exp(FE_{ACh}/RT))/([K^+]_i \exp(FE_{ACh}/RT) - [K^+]_o) = 1.83 \quad (1)$$

where $[Na^+]_o$ and $[Na^+]_i$ are the extracellular and intracellular concentrations of Na^+, and $[K]_o$ and $[K^+]_i$ are the extracellular and intracellular concentrations of K^+, respectively. Bath application of low-Na^+ solution shifted the steady-state *I-V* curve to the left and changed the reversal potential to −47 mV (Fig. 6B, *n* = 3). The calculated value of reversal potential according to the Goldman-Hodgkin-Katz voltage equation is −48.2 mV, assuming only Na^+ and K^+ ions contribute to the CCh-induced current with P_k/P_{Na} = 1.83. The reversal potential was unaffected by bath application of low Cl^- solution (70 mM Cl^-, NaCl was substituted by Na-isethionate) (Fig. 6C, *n* = 5). This suggests that Cl ions are not involved in the CCh-induced inward current.

Discussion

ACh affects the oscillatory and repetitive firing properties of neurons (Gola et al. 1998; Klink and Alonso 1997a; McCormick and Prince 1986b). ACh and its agonists increase respiratory frequency in vivo (Burton et al. 1997; Gesell et al. 1943; Weinstock et al. 1981) and in the en bloc brain stem-spinal cord preparation in vitro (Monteau et al. 1990; Murakoshi et al. 1985). In this study, we describe the actions of ACh (and its agonists) on respiratory-related motor pattern in a medullary slice preparation and on inspiratory neurons in the preBötC, its pharmacology, and its ionic mechanisms. Our principal finding is that in preBötC inspiratory neurons, ACh acts via M3-like receptors on the postsynaptic neurons to open a cationic channel permeable to Na^+ and K^+. This resultant inward cation current depolarizes inspiratory neurons including pacemaker neurons. It has been hypothesized that pacemaker(-like) neurons in preBötC are the kernel for respiratory rhythm generation (Feldman and Smith 1989; Feldman et al. 1990; Smith et al. 1991), and the voltage-dependent bursting properties of the pacemaker neurons underlie respiratory frequency regulation (Koshiya and Smith 1999). We showed that when the membrane potentials of inspiratory and pacemaker neurons were modulated by cholinergic agents, the respiratory frequency was altered correspondingly. These results are consistent with the pacemaker hypothesis. Our results do not exclude the possibility of presynaptic effects of ACh on preBötC respiratory neurons through presynaptic muscarinic and/or nicotinic receptors.

Possible role of premotoneurons and hypoglossal motoneurons

We observed that muscarine induced seizure-like activity in XIIn with no corresponding activity in simultaneously recorded preBötC inspiratory neurons (Fig. 1B). We also observed an increase in the amplitude of inspiratory bursts in XIIn, while the amplitude of inspiratory drive recorded from the inspiratory neurons decreased and their action potential frequency was unaffected. These seizures differ from those induced under similar conditions by bicuculline where seizurelike activity is seen in both XIIn and respiratory neurons in preBötC (Shao and Feldman 1997). The muscarine-induced seizure-like activity and the increase of inspiratory amplitude may be due to excitatory effects of muscarine at the motoneu-ron or premotoneuron level outside the preBötC. The various changes in respiratory-related motor output recorded from XIIn may result from the combined effects of muscarine on the central rhythm generator and on the hypoglossal motoneurons. We identified, by simultaneously recording from inspiratory neurons, that cholinergic agents had effects on the rhythm generator in preBötC, and differentiated the roles of the pre-BötC inspiratory neurons and of the premotoneurons or hypo-glossal motoneurons in cholinergic regulation of the respiratory pattern.

Pharmacology of muscarinic receptor subtype

Five subtypes of muscarinic receptors, m1–m5, have been identified by cDNA cloning (Bonner et al. 1987, 1988; Hulme et al. 1990; Kubo et al. 1986). They correspond to the pharmacologically characterized subtype M1–M5 in animal tissues (Caulfield and Birdsall 1998; Lazareno et al. 1990, Waelbroeck et al. 1990). The affinity profiles of subtype specific antagonists were characterized by expressing the five cloned receptors in Chinese hamster ovary (CHO) cells (Dörje et al.1991; Lazareno and Birdsall 1993). None of the tested antagonists is specific for a single subtype, whereas each receptor displayed a unique antagonist binding profile. Characterizing subtypes of muscarinic receptors functionally in neurons in brain slices is difficult compared with isolated neurons because the agonist concentration applied by pressure ejection cannot be measured accurately. Although the concentration is known with bath application, the effect is very slow due to the time it takes for the agonists to diffuse through the tissue to the recorded neurons; during this time, agonist-induced desensitization may occur (Bünemann and Hosey 1999). Our data show that the response of preBötC inspiratory neurons to local application of ACh or CCh, at least at high concentration, is desensitized (Fig. 2). This prevents accurate estimates for dose-response curves and antagonist affinity parameters. In this study, the ACh-induced inward current in the preBötC inspiratory neurons (including pacemaker neurons) was blocked by 4-DAMP (Fig. 4, A and B). Because 4-DAMP exhibits similar affinity to m1 and m3 receptors (Doods et al. 1987; Dörje et al. 1991), we also tested other antagonists: gallamine (selective for the m2 receptor), himbacine (similar affinity to both the m2 and m4 receptors), and pirenzepine (very potent at m1 receptors) (Doods et al. 1987; Dörje et al. 1991; Lazareno and Birdsall 1993). They each had little effect on CCh-induced inward current, suggesting that this 4-DAMP-sensitive ACh-induced response in preBötC inspiratory neurons is not mediated by M1, M2, or M4 receptors. It is most likely primarily mediated by M3-like receptors (Fig. 4, A and C). Of course, we cannot rule out the possibility of coexpression of m1, m2, m4, or m5 receptors in these neurons. The genetic subtype of the receptors should be confirmed by molecular biological methods. Our result is consistent

with that of Nattie and Li (1990) from anesthetized cats, who concluded that respiratory regulation by ACh involved predominantly M3 receptors, whereas cardiovascular regulation involved the M2 subtype.

Ionic mechanism of muscarinic receptor-mediated response

The excitatory effect of muscarinic receptor activation in neurons has been attributed to switching off one or more K^+ currents such as: M current (Brown and Adams 1980; Coggan et al. 1994; McCormick and Prince 1986a), Ca^{2+}-activated K^+ current (Madison et al. 1987; McCormick and Prince 1986a), inward rectifier K^+ current (Uchimura and North 1990; Wang and McKinnon 1996), and a "leak current" (Benson et al. 1988). Excitatory effects of muscarinic receptors mediated by opening channels have been reported recently including: voltage-sensitive Na^+ current (Delmas et al. 1996; Gola et al. 1998), nonselective cation current (Guérineau et al. 1995; Haj-Dahmame and Andrade 1996; Shen and North 1992), and Ca^{2+}-dependent cation current (Fraser and MacVicar 1996; Klink and Alonso 1997b). We found that activation of muscarinic receptors in preBötC inspiratory neurons at resting potential induced an inward current with an increase in membrane conductance. The current was linear in the voltage range between -110 and -20 mV and reversed at -11.4 mV. A high concentration of EGTA or BAPTA in the patch electrode had no effect on this current. A bath solution containing a low concentration of Na^+ shifted the *I-V* curve for this current to the left and shifted the reversal potential to -47 mV, which matched the value calculated with the Goldman equation (Goldman 1943; Hodgkin and Katz 1949) if we assume the channel is permeable to both Na^+ and K^+ ions. A bath solution containing a low concentration of Cl^- did not shift the reversal potential of this current. Thus activation of muscarinic receptors in preBötC inspiratory neurons appears to open a nonselective cation channel permeable to both Na^+ and K^+, which is neither Ca^{2+} nor voltage dependent in the range of -110 to -20 mV. The characteristics of this current resemble the ACh-activated nonselective cation current in CA3 pyramidal neurons in rat hippocampus (Guérineau et al. 1995). This kind of muscarine-activated cation current also is observed in rat locus coeruleus neurons (Shen and North 1992) and in canine pyloric circular muscle cells (Vogalis and Sanders 1990). CCh also induced a slowly activated current at the voltages more positive than -20 mV in preBötC inspiratory neurons (Fig. 3C iii, -10-mV voltage trace). Multiple channels presumably are involved here (Shao and Feldman 1998).

Acknowledgments

References

Benson DM, Blitzer RD, Landau EM. An analysis of depolarization produced in guinea-pig hippocampus by cholinergic receptor stimulation. J Physiol (Lond). 1988; 404:479–496. [PubMed: 3253439]

Böhmer G, Schmid K, Baumann M. Evidence for a respiration-modulated cholinergic action on the activity of medullary respiration-related neurons in the rabbit. An iontophoretic study. Pflügers Arch Arch Eur J Physiol. 1989; 415:72–80. [PubMed: 2576119]

Böhmer G, Schmid K, Schmidt P, Stehle J. Cholinergic effects on spike-density and burst-duration of medullary respiration-related neurones in the rabbit: an iontophoretic study. Neuropharmacology. 1987; 26:1561–1572. [PubMed: 3431661]

Bonner TI, Buckley NJ, Young AC, Brann MR. Identification of a family of muscarinic acetylcholine receptor genes. Science. 1987; 237:527–532. [PubMed: 3037705]

Bonner TI, Young AC, Brann MR, Buckley NJ. Cloning and expression of the human and rat m5 muscarinic acetylcholine receptor genes. Neuron. 1988; 1:403–410. [PubMed: 3272174]

Bradley PB, Lucy AP. Cholinoceptive properties of respiratory neurones in the rat medulla. Neuropharmacology. 1983; 22:853–858. [PubMed: 6621815]

Brown DA, Adams PR. Muscarinic suppression of a novel voltage-sensitive K^+ current in a vertebrate neurone. Nature. 1980; 283:673–676. [PubMed: 6965523]

Bünemann M, Hosey MM. G-protein coupled receptor kinases as modulators of G-protein signalling. J Physiol (Lond). 1999; 517:5–23. [PubMed: 10226145]

Burton MD, Johnson DC, Kazemi H. The central respiratory effects of acetylcholine vary with CSF pH. J Auton Nerv Syst. 1997; 62:27–32. [PubMed: 9021646]

Burton MD, Nouri K, Baichoo S, Samuels-Toyloy N, Kazemi H. Ventilatory output and acetylcholine: perturbations in release and muscarinic receptor activation. J Appl Physiol. 1994; 77:2275–2284. [PubMed: 7868445]

Burton MD, Nouri M, Kazemi H. Acetylcholine and central respiratory control: perturbations of acetylcholine synthesis in the isolated brainstem of the neonatal rat. Brain Res. 1995; 670:39–47. [PubMed: 7719722]

Caulfield MP, Birdsall NJM. International union of pharmacology. XVII. Classification of muscarinic acetylcholine receptors. Pharmacol Rev. 1998; 50:279–290. [PubMed: 9647869]

Coggan JS, Purnyn SL, Knoper SR, Kreulen DL. Muscarinic inhibition of two potassium currents in guinea-pig prevertebral neurons: differentiation by extracellular cesium. Neuroscience. 1994; 59:349–361. [PubMed: 8008197]

Connelly CA, Dobbins EG, Feldman JL. Pre-Bötzinger complex in cats: respiratory neuronal discharge patterns. Brain Res. 1992; 590:337–340. [PubMed: 1422843]

Delmas P, Niel JP, Gola M. Muscarinic activation of a novel voltage-sensitive inward current in rabbit prevertebral sympathetic neurons. Eur J Neurosci. 1996; 8:598–610. [PubMed: 8963452]

Dev NB, Loeschcke HH. A cholinergic mechanism involved in the respiratory chemosensitivity of the medulla oblongata in the cat. Pflügers Arch. 1979; 379:29–36. [PubMed: 571102]

Doods HN, Mathy MJ, Davidesko D, Van Charldorp KJ, De Jonge A, Van Zwieten PA. Selectivity of muscarinic antagonists in radioligand and in vivo experiments for the putative M1, M2 and M3 receptors. J Pharmacol Exp Ther. 1987; 242:257–262. [PubMed: 3612532]

Dörje F, Wess J, Lambrecht G, Tacke R, Mutschler E, Brann MR. Antagonist binding profiles of five cloned human muscarinic receptor subtypes. J Pharmacol Exp Ther. 1991; 256:727–733. [PubMed: 1994002]

Feldman JL, Smith JC. Cellular mechanisms underlying modulation of breathing pattern in mammals. Ann NY Acad, Sci. 1989; 563:114–130. [PubMed: 2476055]

Feldman JL, Smith JC, Elenberger HH, Connelly CA, Liu G, Greer JJ, Lindsay AD, Otto MR. Neurogenesis of respiratory rhythm and pattern: emerging concepts. Am J Physiol Regulatory Integrative Comp Physiol. 1990; 259:R879–R886.

Foutz AS, Boudinot E, Denavit-Saubié M. Central respiratory depression induced by acetylcholinesterase inhibition: involvement of anaesthesia. Eur J Pharmacol. 1987; 142:207–213. [PubMed: 3691638]

Fraser DD, MacVicar BA. Cholinergic-dependent plateau potential in hippocampal CA1 pyramidal neurons. J Neurosci. 1996; 16:4113–4128. [PubMed: 8753873]

Fukuda Y, Loeschcke HH. A cholinergic mechanism involved in the neuronal excitation by H+ in the respiratory chemosensitive structures of the ventral medulla oblongata of rats in vitro. Pflügers Arch. 1979; 379:125–135. [PubMed: 34826]

Funk GD, Smith JC, Feldman JL. Generation and transmission of respiratory oscillations in medullary slices: role of excitatory amino acids. J Neurophysiol. 1993; 70:1497–1515. [PubMed: 8283211]

Gesell R, Hansen ET, Worzniak JJ. Humoral intermediation of nerve cell activation in the central nervous system. Am J Physiol. 1943; 138:776–791.

Gillis RA, Walton DP, Quest JA, Namath IJ, Hamosh P, Dretchen KL. Cadiorespiratory effects produced by activation of cholinergic muscarinic receptors on the ventral surface of the medulla. J Pharmacol Exp Therap. 1988; 247:765–773. [PubMed: 3183970]

Gola M, Delmas P, Chagneux H. Encoding properties induced by a persistent voltage-gated muscarinic sodium current in rabbit sympathetic neurones. J Physiol (Lond). 1998; 510:387–399. [PubMed: 9705991]

Goldman DE. Potential impedance and rectification in membranes. J Gen Physiol. 1943; 27:37–60. [PubMed: 19873371]

Gonsalves SF, Borison HL. Atropine-resistant central respiratory stimulation by bethanechol in cats. J Pharmacol Exp Ther. 1980; 214:297–305. [PubMed: 6771391]

Gray PA, Rekling JC, Bocchiaro CM, Feldman JL. Modulation of respiratory frequency by peptidergic input to rhythmogenic neurons in the preBötzinger complex. Science. 1999; 286:1566–1568. [PubMed: 10567264]

Guérineau NC, Bossu JL, Gähwiler BH, Gerber U. Activation of a nonselective cationic conductance by metabotropic glutamatergic and muscarinic agonists in CA3 pyramidal neurons of the rat hippocampus. J Neurosci. 1995; 15:4395–4407. [PubMed: 7790916]

Haj-Dahmame S, Andrade R. Muscarinic activation of a voltage-dependent cation nonselective current in rat association cortex. J Neurosci. 1996; 16:3848–3861. [PubMed: 8656279]

Haji A, Furuichi S, Takeda R. Effects of iontophoretically applied acetylcholine on membrane potential and synaptic activity of bulbar respiratory neurones in decerebrate cats. Neuropharmacology. 1996; 35:195–203. [PubMed: 8734489]

Haxhiu MA, Mitra J, Van Lunteren E, Bruce EN, Cherniack NS. Hypoglossal and phrenic responses to cholinergic agents applied to ventral medullary surface. Am J Physiol Regulatory Integrative Comp Physiol. 1984; 247:R939–R944.

Hodgkin AL, Katz B. The effect of sodium ions on the electrical activity of the giant axon of the squid. J Physiol (Lond). 1949; 108:37–77. [PubMed: 18128147]

Hulme EC, Birdsall NJ, Buckley NJ. Muscarinic receptor subtypes. Annu Rev Pharmacol Toxicol. 1990; 30:633–673. [PubMed: 2188581]

Johnson SM, Smith JC, Funk GD, Feldman JL. Pacemaker behavior of respiratory neurons in medullary slices from neonatal rat. J Neurophysiol. 1994; 72:2598–2608. [PubMed: 7897477]

Jordan D, Spyer KM. Effects of acetylcholine on respiratory neurones in the nucleus ambiguus-retroambigualis complex of the cat. J Physiol (Lond). 1981; 320:103–111. [PubMed: 7320931]

Kinney HC, Filliano JJ, Sleeper LA, Mandell F, Valdes-Dapena M, White WF. Decreased muscarinic receptor binding in the arcuate nucleus in sudden infant death syndrome. Science. 1995a; 269:1446–1450. [PubMed: 7660131]

Kinney HC, Panigrahy A, Rava LA, White WF. Three-dimensional distribution of [^{3}H]quinuclidinyl benzilate binding to muscarinic cholinergic receptors in the developing human brainstem. J Comp Neurol. 1995b; 362:350–367. [PubMed: 8576444]

Kirsten EB, Satayavivad J, St John WM, Wang SC. Alteration of medullary respiratory unit discharge by iontophoretic application of putative neurotransmitters. Br J Pharmacol. 1978; 63:275–281. [PubMed: 27271]

Klink R, Alonso A. Muscarinic modulation of the oscillatory and repetitive firing properties of entorhinal cortex layer II neurons. J Neurophysiol. 1997a; 77:1813–1828. [PubMed: 9114238]

Klink R, Alonso A. Ionic mechanisms of muscarinic depolarization in entorhinal cortex layer II neurons. J Neurophysiol. 1997b; 77:1829–1843. [PubMed: 9114239]

Koshiya N, Guyenet PG. Tonic sympathetic chmoreflex after blockade of respiratory rhythmogenesis in the rat. J Physiol (Lond). 1996; 491:859–869. [PubMed: 8815217]

Koshiya N, Smith JC. Neuronal pacemaker for breathing visualized in vitro. Nature. 1999; 400:360–363. [PubMed: 10432113]

Kubo T, Fukuda K, Mikami A, Maeda A, Takahashi H, Mishina M, Haga T, Haga K, Ichiyama A, Kangawa K, Kojima M, Matsuo H, Hirose T, Numa S. Cloning, sequencing and expression of

complementary DNA encoding the muscarinic acetylcholine receptor. Nature. 1986; 323:411–416. [PubMed: 3762692]

Lazareno S, Birdsall NJ. Pharmacological characterization of ace-tylcholine-stimulated [^{35}S]-GTP gamma S binding mediated by human muscarinic m1–m4 receptors: antagonist studies. Br J Pharmacol. 1993; 109:1120–1127. [PubMed: 8401923]

Lazareno S, Buckley NJ, Roberts FF. Characterization of muscarinic M4 binding sites in rabbit lung, chicken heart, and NG108–15 cells. Mol Pharmacol. 1990; 38:805–815. [PubMed: 2250662]

Lotti M. Treatment of acute organophosphate poisoning. Med J Aust. 1991; 154:51–55. [PubMed: 1984587]

Madison DV, Lancaster B, Nicoll RA. Voltage clamp analysis of cholinergic action in the hippocampus. J Neurosci. 1987; 7:733–741. [PubMed: 3559710]

Mallios V, Lydic R, Baghdoyan HA. Muscarinic receptor subtypes are differentially distributed across brain stem respiratory nuclei. Am J Physiol Lung Cell Mol Physiol. 1995; 268:L941–L949.

McCormick DA, Prince DA. Mechanisms of action of acetylcholine in the guinea-pig cerebral cortex in vitro. J Physiol (Lond). 1986a; 375:169–194. [PubMed: 2879035]

McCormick DA, Prince DA. Acetylcholine induces burst firing in thalamic reticular neurones by activating a potassium conductance. Nature. 1986b; 319:402–405. [PubMed: 2418361]

Metz B. Brain acetylcholinesterase and a respiratory reflex. Am J Physiol. 1958; 192:101–105. [PubMed: 13498158]

Monteau R, Morin D, Hilaire G. Acetylcholine and central chemosensitivity: in vitro study in the newborn rat. Respir Physiol. 1990; 81:241–253. [PubMed: 2263784]

Murakoshi T, Suzue T, Tamai S. A pharmacological study on respiratory rhythm in the isolated brainstem-spinal cord preparation of the newborn rat. Br J Pharmacol. 1985; 86:95–104. [PubMed: 2413943]

Nattie EE, Li A. Ventral medulla sites of muscarinic receptor subtypes involved in cardiorespiratory control. J Appl Physiol. 1990; 69:33–41. [PubMed: 2118496]

Nattie EE, Wood J, Mega A, Goritski W. Rostral ventrolateral medulla muscarinic receptor involvement in central ventilatory chemosensitivity. J Appl Physiol. 1989; 66:1462–1470. [PubMed: 2496097]

Ramirez JM, Quellmalz UJA, Richter DW. Postnatal changes in the mammalian respiratory network as revealed by the transverse brainstem slice of mice. J Physiol (Lond). 1996; 491:799–812. [PubMed: 8815212]

Ramirez JM, Schwarzacher SW, Pierrefiche O, Olivera BM, Richter DW. Selective lesioning of the cat pre-Bötzinger complex in vivo eliminates breathing but not gasping. J Physiol (Lond). 1998; 507:895–907. [PubMed: 9508848]

Rekling JC, Feldman JL. Calcium-dependent plateau potentials in rostral ambiguus neurons in the newborn mouse brain stem in vitro. J Neurophysiol. 1997; 78:2483–2492. [PubMed: 9356399]

Rekling JC, Feldman JL. PreBötzinger complex and pacemaker neurons: hypothesized site and kernel for respiratory rhythm generation. Annu Rev Physiol. 1998; 60:385–405. [PubMed: 9558470]

Salmoiraghi GC, Steiner FA. Acetylcholine sensitivity of cat's medullary neurons. J Neurophysiol. 1963; 26:581–597. [PubMed: 13991142]

Schwarzacher SW, Smith JC, Richter DW. PreBötzinger complex in the cat. J Neurophysiol. 1995; 73:1452–1461. [PubMed: 7643160]

Shao XM, Feldman JL. Respiratory rhythm generation and synaptic inhibition of expiratory neurons in preBötzinger complex: differential roles of glycinergic and GABAergic neural transmission. J Neurophysiol. 1997; 77:1853–1860. [PubMed: 9114241]

Shao XM, Feldman JL. Modulation of respiratory pattern by acetylcholine (ACh): postsynaptic effects on preBötzinger complex (preBötC) inspiratory neurons mediated by muscarinic M3 receptors. Soc Neurosci Abstr. 1998; 24:519.

Shen KZ, North RA. Muscarine increases cation conductance and decreases potassium conductance in rat locus coeruleus neurones. J Physiol (Lond). 1992; 455:471–485. [PubMed: 1484360]

Smith JC, Ellenberger HH, Ballanyi K, Richter DW, Feldman JL. Pre-Bötzinger complex: a brainstem region that may generate respiratory rhythm in mammals. Science. 1991; 254:716–719. [PubMed: 1948051]

Solomon IC, Edelman NG, Neubauer JA. Patterns of phrenic motor output evoked by chemical stimulation of neurons located in the preBötzinger complex in vivo. J Neurophysiol. 1999; 81:1150–1161. [PubMed: 10085342]

Uchimura N, North RA. Muscarine reduces inwardly rectifying potassium conductance in rat nucleus accumbens neurones. J Physiol (Lond). 1990; 422:369–380. [PubMed: 1693682]

Vogalis F, Sanders KM. Cholinergic stimulation activates a non-selective cation current in canine pyloric circular muscle cells. J Physiol (Lond). 1990; 429:223–236. [PubMed: 1703570]

Waelbroeck M, Tastenoy M, Camus J, Christophe J. Binding of selective antagonists to four muscarinic receptors (M1 to M4) in rat forebrain. Mol Pharmacol. 1990; 38:267–273. [PubMed: 2385234]

Wang HS, MeKinnon D. Modulation of inwardly rectifying currents in rat sympathetic neurones by muscarinic receptors. J Physiol (Lond). 1996; 492:467–478. [PubMed: 9019543]

Weinstock M, Roll D, Zilberman Y. An analysis of the respiratory stimulant effect of physostigmine and neostigmine in the conscious rabbit. Clin Exp Pharmacol Physiol. 1981; 8:151–158. [PubMed: 6788414]
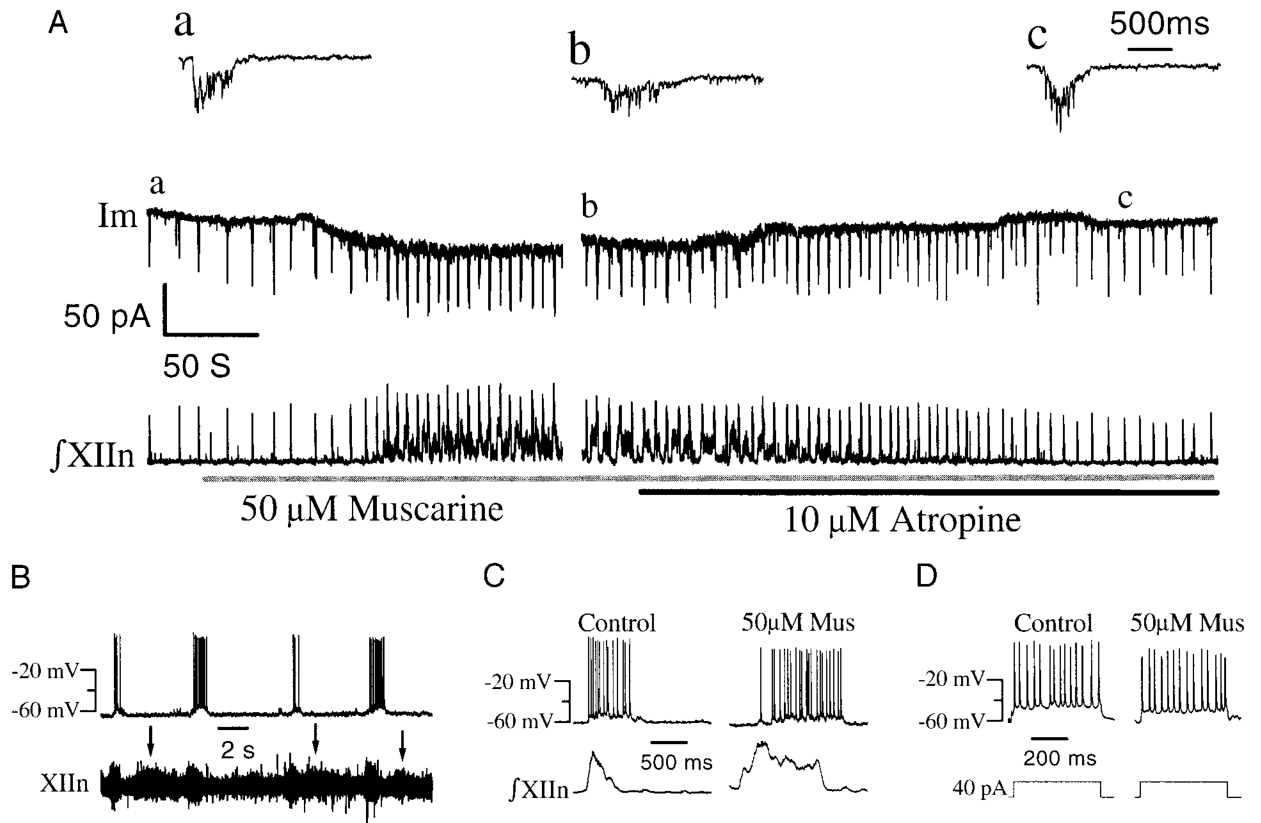
Fig. 1.
Effects of muscarine on respiratory pattern and inspiratory neurons. *A*: simultaneous recordings from XIIn and a preBötzinger complex (preBötC) inspiratory neuron before and during bath application of 50 μM muscarine and then 10 μM atropine. Inspiratory neuron was voltage clamped at −60 mV. XIIn signal was integrated. *Insets, a–c*: averages of 5 consecutive inspiratory drives in extended time scale picked from corresponding *a–c* of the whole cell recording. Averages were triggered by the rising phase of the inspiratory bursts from XIIn. *B*: seizure-like activity (indicated by ↓) from XIIn (unintegrated) induced by 50 μM muscarine and concurrent activity of inspiratory neuron under current clamp at −64 pA. *C*: muscarine affected number of action potentials per inspiratory drive in the inspiratory neuron under current clamp. *D*: muscarine affected number of action potentials per current command pulse (40 pA, 500 ms; same neuron as *C*).
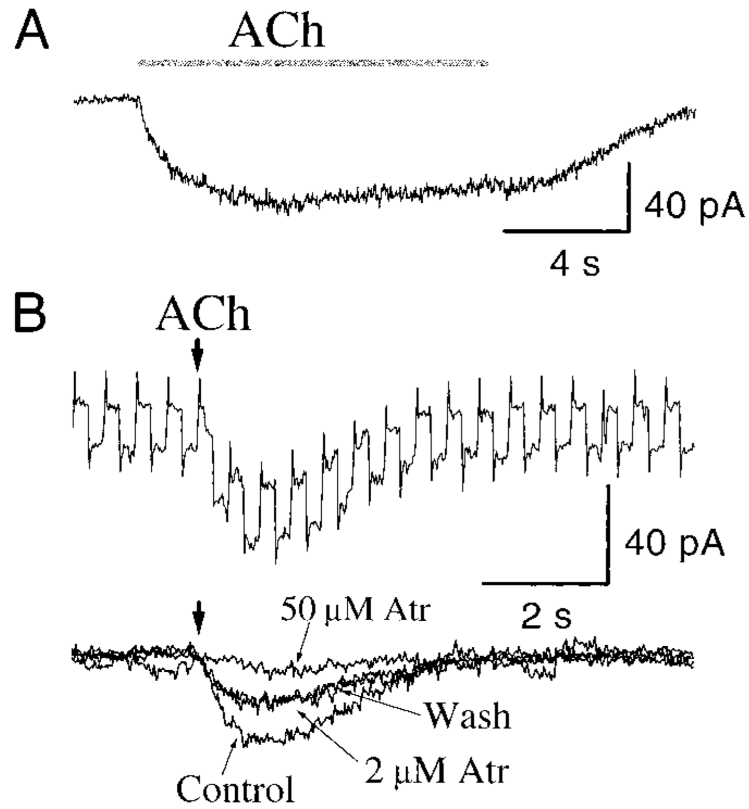
Fig. 2.
Responses of preBötC inspiratory neurons to local application of 2 mM ACh. *A*: application of ACh (10 s) induced a tonic inward current under voltage clamp at −60 mV. *B*: membrane conductance change induced by a short ACh ejection (200-ms pressure pulse) measured by applying a series of −5 mV voltage clamp pulses (*top*). ACh-induced responses during bath application of 2 μM, 50 μM atropine (Atr), and the response after 7 min wash with standard recording solution (*bottom*). Bath solution contained 0.5 μM TTX.
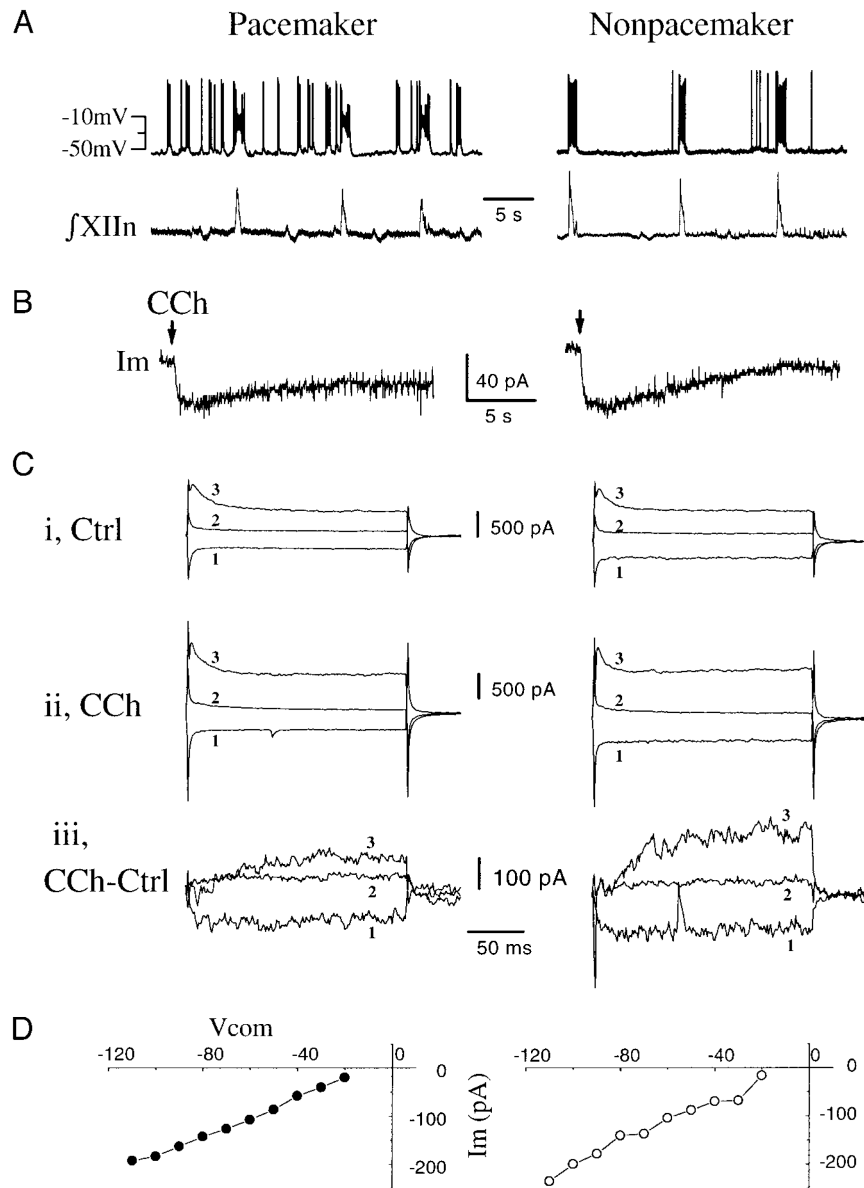
Fig. 3.
Effects of local application of CCh on a pacemaker and a nonpacemaker inspiratory neuron. *A*: firing behavior of pacemaker (current clamp at −15 pA) and nonpacemaker neuron (current clamp at −40 pA). *B*: 250-ms local application of 2 mM carbachol (CCh, ↓) induced inward currents in both neuron (voltage clamp at −60 mV; bath solution contained 0.5 μM TTX). *C*: selected traces of whole cell current under voltage clamp step pulses (200 ms) from a holding potential of −65 mV to −110 (*trace 1*), −40 (*trace 2*), and −10 mV (*trace 3*) for the pacemaker and nonpacemaker neurons: *i,* Control; *ii,* during CCh application; *iii,* subtraction of control from CCh trace. *D*: *I-V* relations of CCh-induced responses in pacemaker and nonpacemaker neurons obtained by subtraction of the steady-state current of control *I-V* curve from that during CCh application.
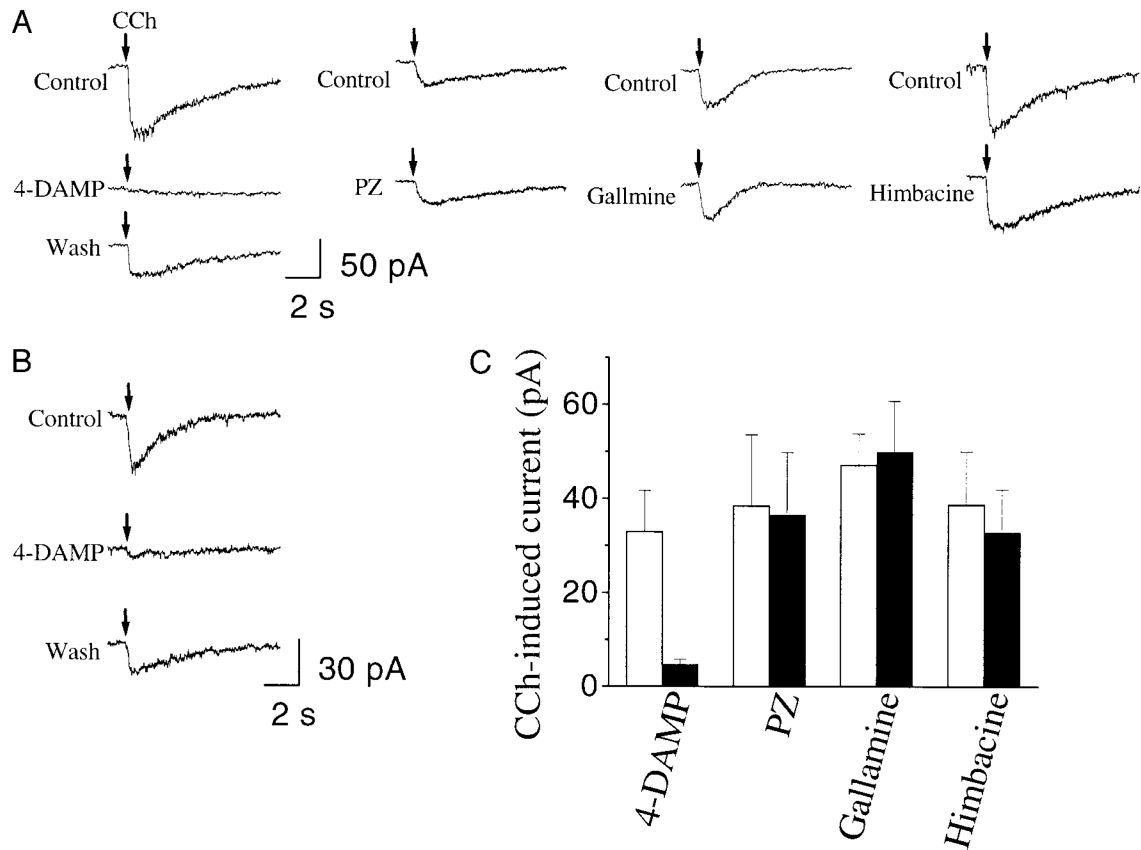
Fig. 4.
Pharmacology of the CCh-induced inward current in preBötC inspiratory neurons. *A*: effects of 10 μM 4-diphenylacetoxy-*N*-methylpiperidine methiodide (4-DAMP), 1 μM pirenzepine (PZ), 10 μM gallamine, or 10 μM himbacine on CCh-induced currents (voltage clamp at −60 mV). ↓, onset of 150–250 ms pressure application of 2 mM CCh around the neurons. *B*: effect of 4-DAMP on CCh-induced current in a pacemaker neuron. *C*: summary of the effects (■) of 4-DAMP (*n* = 6), PZ (*n* = 6), gallamine (*n* = 3), and himbacine (*n* = 5) vs. their control (□). Each bar represents mean ± SE.
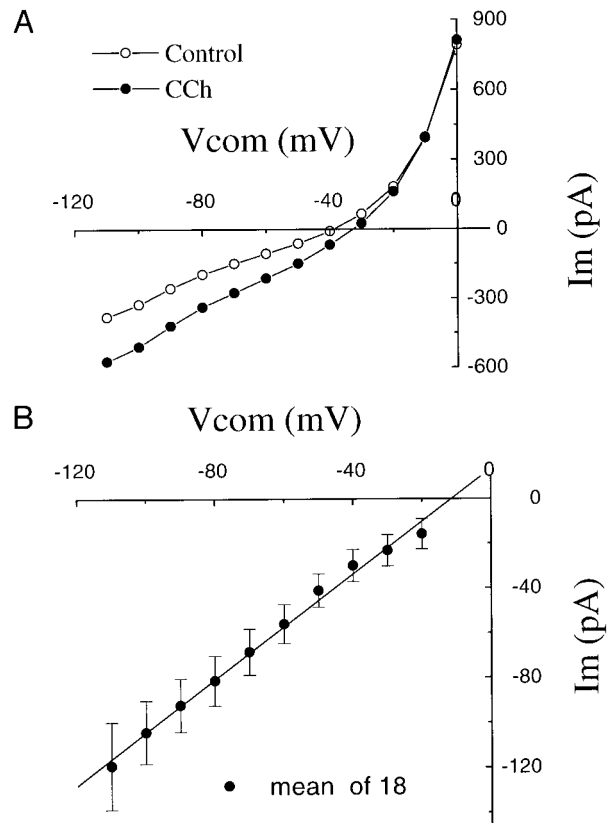
Fig. 5.
A: steady-state *I-V* relation of preBötC inspiratory neuron under control conditions (○) and during local application of CCh (●). Under voltage clamp holding at −65 mV, a series of 200-ms voltage command pulses from −110 to 0 mV was applied. Currents were measured at ∼190 ms. *B*: *I-V* relation for CCh. *I-V* relation for CCh was obtained by subtracting the *I-V* curve for control conditions from that during CCh application. Each symbol is the mean of 18 neurons, the error bar is SE. —, linear regression of the *I-V* data. Extrapolated regression line at point *Im* = 0 is *V* = −11.4 mV.
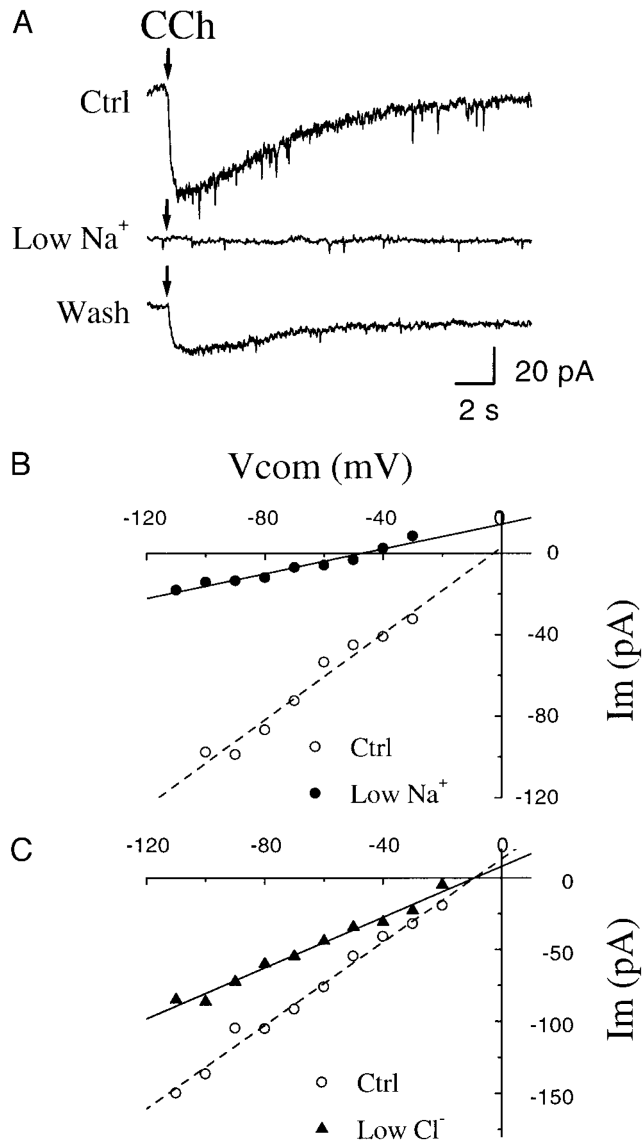
Fig. 6.
Effects of ionic substitution on CCh-induced response in preBötC inspiratory neurons. *A*: local injections of 2 mM CCh (↓) induced inward currents (voltage clamp at −65 mV) under control (Ctrl) conditions, during bath application of low Na^+ (24 mM; 128 mM of NaCl was substituted by Tris-Cl) solution and after wash with standard recording solution. *B*: *I-V* relation of CCh-response in the control condition and during bath application of low Na^+ solution. Symbols represent means from 3 neurons; lines are linear regression of data. *C*: *I-V* relations of CCh-response under control condition and during bath application of low Cl^- solution (70 mM, 70 mM of NaCl was substituted by Na-isethionate). Symbols represent means of 5 neurons. Straight lines are the linear regression of data.

Table 1

Effects of muscarine on XIIn motor output and on preBötC inspiratory neurons

	Control	50 μM Muscarine	Percent Control, %	n	P Value
XIIn motor output					
Respiratory frequency, min^{-1}	5.7 ± 2.1	8.1 ± 1.4	150.3 ± 33.5	7	0.0052
Inspiratory duration, ms	596.6 ± 166.9	1259.6 ± 685.4	209.5 ± 90.1	7	0.029
Inspiratory amplitude, μV	123.4 ± 42.8	167.9 ± 68.1	134.0 ± 31.6	7	0.015
PreBötC neurons					
Phasic inward current duration, ms	726.0 ± 194.4	1181.8 ± 430.4	166.6 ± 59.9	6	0.029
Phasic inward current amplitude, pA	67.9 ± 31.6	41.9 ± 24.4	60.6 ± 14.0	6	0.012
No. of action potentials per inspiration	14.7 ± 7.7	18.4 ± 8.7	130.9 ± 20.4	5	0.024
No. of action potentials per current pulse	15.8 ± 3.7	15.9 ± 10.3	101.8 ± 17.8	5	0.95

XIIn indicates hypoglossal nerve root. Numbers are means ± SD. n is number of cells [for preBötzinger Complex (preBötC) inspiratory neurons] or number of slices (for XIIn motor output). Respiratory frequency was averaged for 3 min both for control condition and during bath application muscarine for each cell. For all other measurements (except the number of action potentials/current pulse), we averaged 5–8 respiratory periods both for control and during muscarine for each cell. P values were from paired t-tests taking the measurements during muscarine vs. control of the same cell or same slice (for motor output measurements) as pairs. The phasic inward currents were measured under voltage clamp at −60 mV. The number of action potentials per current pulse was measured under current clamp keeping the membrane potential near −60 mV and applying 40 pA, 200 ms square pulses.